Unshielded three-axis vector operation of a spin-exchange-relaxation-free atomic magnetometer

S. J. Seltzer[a] and M. V. Romalis
Department of Physics, Princeton University, Princeton, New Jersey 08544

(Received 29 June 2004; accepted 20 September 2004)

We describe a vector alkali–metal magnetometer that simultaneously and independently measures all three components of the magnetic field. Using a feedback system, the total field at the location of the magnetometer is kept near zero, suppressing the broadening due to spin-exchange collisions. The resonance linewidth and signal strength of the magnetometer compare favorably with two different scalar operation modes in which spin-exchange relaxation is only partially suppressed. Magnetic field sensitivity on the order of 1 $\mathrm{pT}/\sqrt{\mathrm{Hz}}$ is demonstrated in a laboratory environment without magnetic shields. © *2004 American Institute of Physics*. [DOI: 10.1063/1.1814434]

Sensitive magnetometers find a wide range of applications in monitoring the Earth's magnetic field, detecting magnetic anomalies, and measuring biological magnetic fields. Traditionally, superconducting quantum interference devices (SQUIDs) have provided the highest sensitivity for magnetometry. Most sensitive atomic magnetometers are competitive with the best SQUIDs[1,2] but do not require cryogenic cooling; they measure the Larmor spin precession in a magnetic field using an optically pumped vapor of alkali-metal[3,4] or helium[5,6] atoms. While SQUID magnetometers are vector detectors that measure the field projection along one particular direction, atomic magnetometers usually operate in the scalar mode, measuring the total magnitude of the magnetic field. Vector atomic magnetometers have been demonstrated by operating near a zero magnetic field[3,7] or by applying magnetic field modulation to different field components in a scalar magnetometer and using lock-in detection.[5]

The fundamental sensitivity limit of an atomic magnetometer due to shot noise is given by $\delta B=(\gamma\sqrt{nVT_2t})^{-1}$, where γ is the gyromagnetic ratio, n is the number density of atoms, V is the measurement volume, T_2 is the transverse spin relaxation time, and t is the measurement time. Practical atomic magnetometers are often limited not by statistical noise, but by various sources of technical noise in the detection of the atomic spin precession. From a purely phenomenological point of view, the magnetometer sensitivity depends on the signal-to-noise ratio (S/N) of the Zeeman resonance signal and on the width of the resonance $\Delta B=(\gamma T_2)^{-1}$,

$$\delta B=\frac{\Delta B}{(\mathrm{S/N})}. \tag{1}$$

Spin-exchange collisions between alkali atoms often limit the sensitivity of atomic magnetometers by causing transverse spin relaxation so that $T_2\sim T_{\mathrm{SE}}=(n\bar{v}\sigma_{\mathrm{SE}})^{-1}$, where $\bar{v}$ is the average thermal velocity and $\sigma_{\mathrm{SE}}\simeq 2\times 10^{-14}$ cm^2 is the spin-exchange cross section. To overcome this limitation, some sensitive magnetometers use large measurement volumes and a low density of atoms.[1,3] Two distinct methods for suppressing spin-exchange broadening have been demonstrated. By operating near zero magnetic field at a high alkali–metal density, one can completely eliminate transverse spin relaxation due to spin-exchange collisions.[8,7] In this regime, $T_2\sim T_{\mathrm{SD}}=(n\bar{v}\sigma_{\mathrm{SD}})^{-1}$, where σ_{SD} is the spin-destruction cross section. For K–K collisions, $\sigma_{\mathrm{SD}}=1\times 10^{-18}$ cm^2, four orders of magnitude smaller than the spin-exchange cross section. In a finite magnetic field, on the other hand, spin-exchange collisions can be partially suppressed by pumping nearly all atoms into the same Zeeman state.[9] In this regime, the pumping rate may be optimized so that $T_2\sim(n\bar{v}\sqrt{\sigma_{\mathrm{SE}}\sigma_{\mathrm{SD}}})^{-1}$.

In this letter, we show that a spin-exchange-relaxation-free (SERF) magnetometer operating near zero field can be used as a three-axis vector magnetic field detector. Using a feedback system to keep the magnetic field at the sensor close to zero, we demonstrate its operation in an unshielded environment. We compare the resonance linewidth and signal strength of the SERF magnetometer to two types of scalar magnetometers operating in a finite magnetic field: one using rf excitation and another using intensity modulation of the pump laser at the Larmor frequency. In both scalar operation modes, the spin-exchange relaxation is partially suppressed by optimizing the optical pumping rate.

The setup of the SERF magnetometer is shown in Fig. 1.

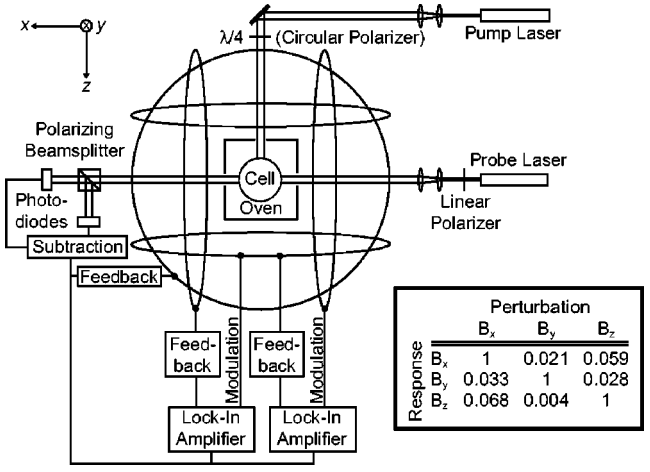

FIG. 1. Setup of the unshielded SERF magnetometer operating in vector mode. Optical rotation of the probe beam is detected using a polarizing beamsplitter oriented at 45° to the beam's initial polarization by subtracting the two photodiode signals. The inset shows the orthogonality of the magnetometer response.

[a]Electronic mail: sseltzer@princeton.edu

The cell containing K atoms, 2.5 atm of ^{4}He as a buffer gas, and 60 Torr of N_2 for quenching is heated to 170 °C by hot air within a glass oven. The ambient magnetic field is cancelled by three pairs of orthogonal Helmholtz coils. To attenuate the high level of 60 Hz noise present in our laboratory environment without affecting the low-frequency and dc components of the magnetic field, the cell is surrounded by 2-in.-thick aluminum plates. A second set of small coils located inside the aluminum shield is used to supply magnetic field modulations. The atoms are pumped along the z direction by a 300–mW diode laser tuned to the $D1$ resonance of K at 770 nm. The S_x component of spin polarization is measured using optical rotation of a 20–mW probe beam propagating along the x direction and tuned 0.5 nm off resonance.

The behavior of the spins is described by a density matrix equation derived in Ref. 10. In the regime of low magnetic field and high alkali–metal density, such that $\gamma|\mathbf{B}|T_{\mathrm{SE}} \ll 1$, this equation can be simplified,[7] and electron spin evolution is described by a Bloch equation

$$\frac{d\mathbf{S}}{dt} = \gamma \mathbf{S} \times \mathbf{B} + R(S_0 \hat{z} - \mathbf{S}) - \frac{\mathbf{S}}{T_2}, \tag{2}$$

where $\gamma = g_s \mu_B / q\hbar$ is the gyromagnetic ratio, R is the pumping rate, $S_0 = sR/2(R + T_1^{-1})$ is the equilibrium electron spin polarization, and $T_2 = T_1 = T_{\mathrm{SD}}$ is the relaxation time due to spin-destruction collisions. Here, $q = 6$ is the slowing-down factor for K ($I = 3/2$), $s \simeq 1$ is the photon polarization of the optical pumping beam, and $g_s \simeq 2$ is the Dirac g-factor. For slowly changing magnetic fields, we can set $d\mathbf{S}/dt = 0$ and obtain

$$S_x = S_0 \frac{\beta_y - \beta_x \beta_z}{1 + (\beta_x^2 + \beta_y^2 + \beta_z^2)}, \tag{3}$$

where we introduced a dimensionless magnetic field parameter $\boldsymbol{\beta} = \gamma \mathbf{B}/(R + T_2^{-1})$. To measure all three magnetic field components, we use Helmholtz coils to add small field modulations along the x and z axes, such that

$$\begin{aligned} \beta_x &= \beta_x^0 + \beta_x^{\mathrm{mod}} \sin(\omega_x t) \\ \beta_z &= \beta_z^0 + \beta_z^{\mathrm{mod}} \sin(\omega_z t), \end{aligned} \tag{4}$$

where β_x^0 and β_z^0 are components of the ambient magnetic field and β_x^{mod} and β_z^{mod} are the modulation amplitudes. The modulation frequencies ω_x and ω_z should be slow enough that the quasi-steady-state solution is valid. In our experiment, we have used modulation frequencies on the order of 100 Hz. If the ambient field and modulation amplitudes are small enough such that $|\beta| \ll 1$, then Eq. (3) may be expanded

$$S_x \approx S_0[\beta_y - \beta_x^0 \beta_z^0 - \beta_x^0 \beta_z^{\mathrm{mod}} \sin(\omega_z t) - \beta_z^0 \beta_x^{\mathrm{mod}} \sin(\omega_x t)]. \tag{5}$$

Thus, to first order, the dc response of the magnetometer is linear in β_y, while lock-in amplifiers referenced to ω_x and ω_z provide signals that are proportional to β_z^0 and β_x^0, respectively. Real-time feedback can be used to adjust the currents in all three Helmholtz coils to keep the magnetic field experienced by the atoms near zero. The compensating currents in the three coils then serve as a measure of the vector components of the magnetic field.

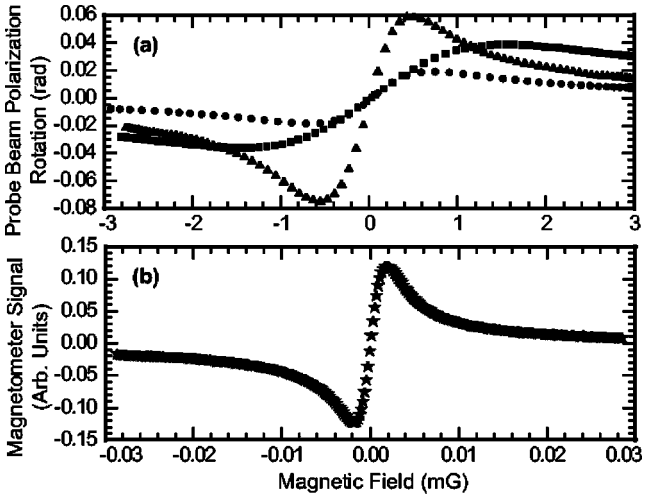

FIG. 2. (a) The dispersion curves obtained near the resonance for a vector SERF magnetometer (triangles) and a scalar magnetometer with rf modulation (squares) or amplitude-modulated pump beam (circles), all in a magnetically unshielded environment. The slopes near the resonance provide the relative intrinsic sensitivities of different magnetometer modes. (b) The dispersion curve obtained from a SERF magnetometer in a magnetically shielded environment with a linewidth of 3.8 μG (see Ref. 7).

We compare the vector SERF operation mode of the magnetometer with two different scalar operation modes. In the first mode, a finite magnetic field is applied along the z direction, parallel to the pumping beam. A weak rf field is applied along the y direction, causing the atomic spins to precess about the z axis. This operation is similar to most scalar atomic magnetometers,[1,4] except that a separate probe laser measures the oscillating S_x component of the spin. A lock-in amplifier is used to measure the optical rotation of the probe beam at the Larmor frequency. In the second scalar mode, a finite magnetic field is applied along the y direction and the pump beam is amplitude modulated at the Larmor frequency, causing the spins to precess about the y axis.[11] The current of the laser diode is modulated with a square wave with a duty cycle of 30%. Reducing the duty cycle below 50% allows the atoms to achieve a higher spin polarization. The oscillating S_x component of the spins is again detected with a lock-in amplifier.

The dispersion resonance signals are shown in Fig. 2(a) for the vector and both scalar modes. For the vector mode, the figure shows the dc optical rotation as a function of the B_y field, while for the scalar modes it shows the out-of-phase signal of the lock-in amplifier as a function of the magnetic field detuning from the Larmor resonance, set to 20 kHz. According to Eq. (1), the magnetometer sensitivity is proportional to the slope of the dispersion curves near the resonance. For each mode various operational parameters, such as the pump beam intensity and the rf modulation amplitude, were optimized to maximize the slope. The density of the alkali atoms and the parameters of the probe beam were kept constant. In our conditions, the slope of the vector magnetometer response is four times greater than that for either of the scalar modes, mainly due to a more complete suppression of the spin-exchange collisions.

The vector magnetometer has a resonance linewidth of 1.0 mG. For comparison, we show in Fig. 2(b) the dispersion signal obtained with the SERF magnetometer in a magnetically shielded environment,[7] which has a resonance linewidth of 3.8 μG. This demonstrates that the sensitivity of the

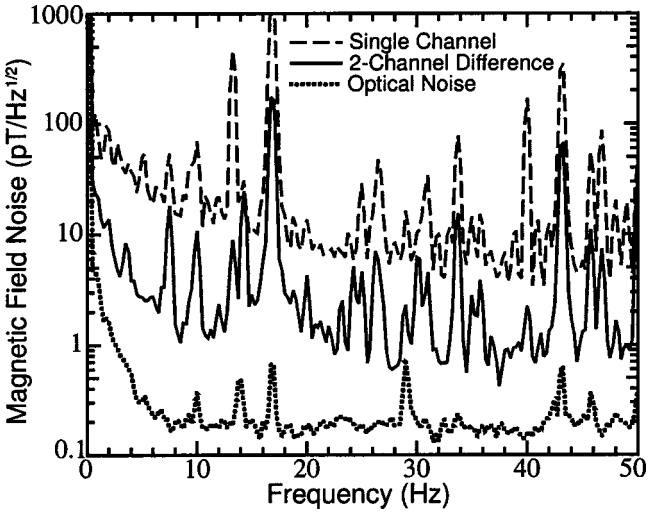

FIG. 3. The spectrum of the magnetic noise in the SERF vector magnetometer for a single channel and the difference of two channels. Also shown is the optical noise obtained in the absence of pumping light.

SERF magnetometer in the unshielded environment can still be greatly improved. In our case, the performance was limited by the presence of the magnetic noise at 60 Hz and its harmonics, which were on the order of 0.2 mG despite the eddy-current shielding by the aluminum plates. It required us to increase the optical pumping rate R well beyond the optimal regime $R \sim T_2^{-1}$ so that the condition $|\beta| \ll 1$ can be satisfied. By operating in a remote location or improving the shielding at high frequencies, one can obtain a substantial increase in the sensitivity of the SERF magnetometer.

In contrast, the scalar magnetometers are operating near the limit of their sensitivity due to spin-exchange collisions. To estimate their optimal sensitivity, we performed a numerical simulation of the rf magnetometer using the density-matrix formalism and including the effect of the rf broadening. Just as for the experimental data, we optimized the slope of the dispersion curve with respect to the optical pumping rate and the strength of the rf excitation. We find that under optimal conditions, the full linewidth of the dispersion curve is equal to $\Delta B \approx 1.7\gamma^{-1}(T_{SE}T_{\mathrm{SD}})^{-1/2}$. In our experiment, $T_{\mathrm{SD}} = 60$ ms and $T_{\mathrm{SE}} = 22\ \mu$s, which gives a linewidth of 0.35 mG, comparable to the measured linewidth in the scalar modes.

With three-axis feedback, we found that the magnetometer is robust against external perturbations, such as moving magnetic objects in its vicinity, and can maintain lock for indefinite intervals of time. The orthogonality of the magnetometer response is shown in the inset of Fig. 1. It is probably limited by the inaccuracies of the modulation fields because the modulation coils were not exactly in the Helmholtz configuration.

The presence of the buffer gas inhibits diffusion of the K atoms enough that atoms located in different parts of the cell independently measure the local magnetic field. The magnetometer can be operated as a gradiometer if the probe beam is detected with multichannel photodiodes, with each channel measuring the magnetic field at a different part of the cell. The spectra of the vector magnetometer noise for the B_y field for a single channel and two-channel difference are shown in Fig. 3. Also displayed is the optical detection noise obtained with the pumping laser blocked, which shows that the magnetometer noise is dominated by the fluctuations of the ambient magnetic field.

In conclusion, we demonstrated the operation of a SERF atomic magnetometer in an unshielded environment, where it exhibits a sensitivity on the order of 1 $\mathrm{pT}/\sqrt{\mathrm{Hz}}$ operating as a gradiometer. By applying small field modulations, the magnetometer can measure all three components of the magnetic field simultaneously. Substantial improvement in sensitivity of the SERF magnetometer is possible by reducing high-frequency magnetic noise as well as magnetic field gradients across the cell.

The authors would like to thank Igor Savukov for assistance with constructing parts of the experiment. This research was funded by the NSF, the Packard Foundation, and Princeton University.

[1] E. B. Aleksandrov, M. V. Balabas, A. K. Vershovskii, A. E. Ivanov, N. N. Yakobson, V. L. Velichanskii, and N. V. Senkov, Opt. Spectrosc. **78**, 292 (1995).
[2] I. K. Kominis, T. W. Kornack, J. C. Allred, and M. V. Romalis, Nature (London) **422**, 596 (2003).
[3] D. Budker, D. F. Kimball, S. M. Rochester, V. V. Yashchuk, and M. Zolotorev, Phys. Rev. A **62**, 043403 (2000).
[4] G. Bison, R. Wynands, and A. Weis, Appl. Phys. B: Lasers Opt. **76**, 325 (2003).
[5] O. Gravrand, A. Khokhlov, J. L. Le Mouël, and J. M. Léger, Earth Planets Space **53**, 949 (2001).
[6] H. Gilles, J. Hamel, and B. Chéron, Rev. Sci. Instrum. **72**, 2253 (2001).
[7] J. C. Allred, R. N. Lyman, T. W. Kornack, and M. V. Romalis, Phys. Rev. Lett. **89**, 130801 (2002).
[8] W. Happer and H. Tang, Phys. Rev. Lett. **31**, 273 (1973).
[9] S. Appelt, A. Ben-Amar Baranga, A. R. Young, and W. Happer, Phys. Rev. A **59**, 2078 (1999).
[10] S. Appelt, A. Ben-Amar Baranga, C. J. Erickson, M. V. Romalis, A. R. Young, and W. Happer, Phys. Rev. A **58**, 1412 (1998).
[11] W. E. Bell and A. L. Bloom, Phys. Rev. Lett. **6**, 280 (1961).